

NASA TT F-9551

GPO PRICE \$ _____

CFSTI PRICE(S) \$ _____

NASA TT F-9551

Hard (1/1/67) 1.00

Microfilm (1/1/67) .50

#653 July 67

CERTAIN RESULTS OF OBSERVATIONS TAKEN DURING
THE SPACE FLIGHT OF THE VOSKHOD

K. Feoktistov, G. Rozenberg, A. Sandomirskiy,
V. Sergeyevich and D. Sonechkin

Translation of "Quelques résultats d'observations effectuées au
cours du vol cosmique du voskhod"
Eight Plenary Meeting and Sixth International Space Science Symposium COSPAR,
Buenos Aires, 10-21 May 1965

N66 31227

FACILITY FORM 802

(ACCESSION NUMBER)

(THRU)

(PAGES)

(CODE)

(NASA CR OR TMX OR AD NUMBER)

(CATEGORY)

NATIONAL AERONAUTICS AND SPACE ADMINISTRATION
WASHINGTON AUGUST 1965

CERTAIN RESULTS OF OBSERVATIONS TAKEN
DURING THE SPACE FLIGHT OF THE
VOSKHOD

K. Feoktistov, G. Rozenberg, A. Sandomirskiy,
V. Sergeyevich and D. Sonechkin

ABSTRACT

Observations performed by the crew of the Voskhod completed experiments begun on the Vostoks. Preliminary results, both photographic and visual, are discussed.

1. Daylight Study of the Structure of the Aureole Surrounding the Earth

In the blue region of the spectrum, studied by colored filters, tropospheric nebulosity has little influence on the structure of the apparent outline of the Earth. A maximum of brilliance is observed in a region near this border. The existence of this maximum conforms to theory.

Figure 3 shows a photometric section of the diurnal horizon, with the perigee shown in abscissa and the brilliance on the ordinate. We can note the abrupt character of the decrease in brilliance in a region corresponding to the apparent optical edge of the Earth, more elevated than the true geometrical horizon. The altitude of the apparent edge is a function of meteorological conditions and of the considered spectral region. This is why, visually, the aureole gradually changes color, passing from white near Earth to blue at high altitudes; it can be observed to an altitude of approximately 30 km.

However, this average effect is perturbed, as was revealed by the flight of the Voskhod, by the presence of atmospheric aerosols, which are observed as clear ~~strips~~ parallel to the horizon.

Figure 4 shows three schematic drawings of the ~~manner of~~ variations of brilliance with altitude. One, two, or three aerosol layers are observed. Altitude x , above the geometrical horizon, is of the order of 10 km. Altitudes z , above the optical horizon, are given in km.

2. The Structure of the Aureole on the Twilight Side.

When the spacecraft is within the Earth's umbra (fig. 5.) sufficiently near the terminator, lighted atmospheric layers are observed to high altitudes. Light diffused by the layers crosses lower layers before reaching the observer; in these layers it undergoes a substantial lessening due to diffusion. Then there exists an aureole which passes in shades from a very clear edge (fig. 6).

In the upper parts of the aureole, as was anticipated from theory, the brilliance diminishes monotonically.

It does so clearly, along the edge, the farther the observer moves from the meridian in which the Sun is located. All of which is a result of the combined effects of anisotropy of diffusion, very strong for small diffusion angles, and of variation of the optical thickness of the layer responsible for the extinction, with the direction of sight.

Vertical photometric sections of the twilight aureole are given in figure 7. Different curves correspond to the various azimuths given in figure 6. The Rayleigh law, in λ^{-4} , makes the low layers practically opaque in blue. Observations of the color of the aureole conform to the qualitative predictions which can be made, considering the effects of Rayleigh diffusion. Figure 8 shows in color the degree of change of color with altitude H .

The thin aerosol layers parallel to the horizon are clearly observed, both from the Vostoks as well as the Voskhods. This is due to the fact that, contrary to observations made from Earth, these layers lie tangentially, with great optical thickness.

In the region between 20 and 25 km, generally two aerosol layers are observed, at close altitudes of 11 and 19 km.

Observations show that the particles composing the aerosols have dimensions exceeding the wavelengths of observed rays. This result agrees with those published by other authors.

3. Nocturnal Horizon of the Earth.

When the spacecraft is on the nocturnal side of the Earth, a slight maximum of brilliance is observed at $2.5 - 3^{\circ}$ from the edge. This effect, discovered by Glenn, has been observed by various astronauts, and observations from Voskhod have confirmed it again. It is shown in diagram in figure 10 (for different cases of nebulosity).

Discussion of the observations shows that the phenomenon, whose physical origin is still unknown, takes place in relatively thin layers.

Certain verifications appear to indicate that it is not an actual atmospheric emission but a diffusion, by an aerosol layer, of lunar light.

The layer considered has been observed clearly in the Southern hemisphere on a polar aurora.

It disappeared just before daybreak, and is invisible after sunrise.

4. Luminous particles Observed Behind the Spacecraft

G. Glenn was first to observe the presence of luminous particles behind the spacecraft. Observed by other astronauts, these particles were also seen by the Voskhod.

These observations led to the following conclusions:

The particles exist objectively and are caused by the spacecraft. The light that they emit comes from the diffusion of solar light, either direct or reflected by Earth (or the craft). Their dimension is of the order of 10μ (if the albedo is 0.2).

After separation from the craft, they follow its trajectory (thus indicating little outside action).

It is difficult to comment on their nature. It is possible that they are particles of Earth dust attached to the craft after its launch. It is also possible that they are pulled from the craft's outer layer by radiation, aerodynamic currents, or micrometeorites.

If we still cannot decide on their physical nature, it is possible that they are responsible for the breakdown of automatic astronavigation equipment.

5. Photographic Observations of the Earth's Cloud Cover

Statistical analysis of results, for various types of clouds, at the periphery of an anticyclone is given by Table I, where the different lines are successively relative to:

1, surface over waters free of cloud cover.

2, $\begin{cases} \text{light nebulosity} \\ \text{Alto-Cumulus (Ac).} \end{cases}$

3, $\begin{cases} \text{heavy nebulosity.} \\ \text{Alto-Cumulus and Cumulus (Ac, Cu).} \end{cases}$

The different columns are defined by the following formulas:

$$m(x) = \frac{1}{n} \sum_{i=1}^n X_i \quad \text{where } X_i = \text{brilliance of the first point of the cloud field;}$$

n = number of points of brilliance;

Other data are: dispersion $D(x)$ of the brilliance; assymetry $\gamma_I(x)$ of brilliance; brilliance excess $\gamma_2(x)$ and $m(\tau_a)$, average duration of passing of certain levels by brilliance.

Results are given in relative units (related to the brilliance logarithms).

Analysis of results shows that most characteristics statistical depend on cloud abundance.

TABLE I

Relative units						kms.				
$m(x)$	$D(x)$	$\gamma_1(x)$	$\gamma_2(x)$	$m(\Delta r)$	$m(r/20)$ [p(20)]	$m(r/30)$ [p(30)]	$m(r/40)$ [p(40)]	$m(r/50)$ [p(50)]	$1/\alpha$	
1)	17,3	1,68	0,60	1,21	0,4	1,6	0,0	0,0	0,0	6,0
						2,3	0,0	0,0	0,0	
2)	21,3	8,61	0,65	0,45	0,8	8,9	2,0	0,0	0,0	8,0
						6,2	0,3	0,0	0,0	
3)	35,8	9,97	0,54	0,26	1,9	-	14,3	7,8	5,2	12,0
							3,6	4,2	1,6	

Table II gives the same statistical parameters to the periphery of a cyclone:

first line { weak nebulosity
Ac

sec nd { heavy nebulosity
Cirrus (Ci)

third { heavy nebulosity
Alto-Cumulus (Ac)

fourth { heavy nebulosity
Ac and Ci.

It can be seen, for example, that average brilliance and brilliance dispersion of a heavy nebulosity of the Cirrus type is clearly weaker than corresponding parameters for Ac.

Normed functions of correlation of brilliance can be considered purely exponential (figs. 11 and 13); solid lines , absence of nebulosity; dashes , weak nebulosity(Ac); mixed, heavy nebulosity (Ac, Cu)/

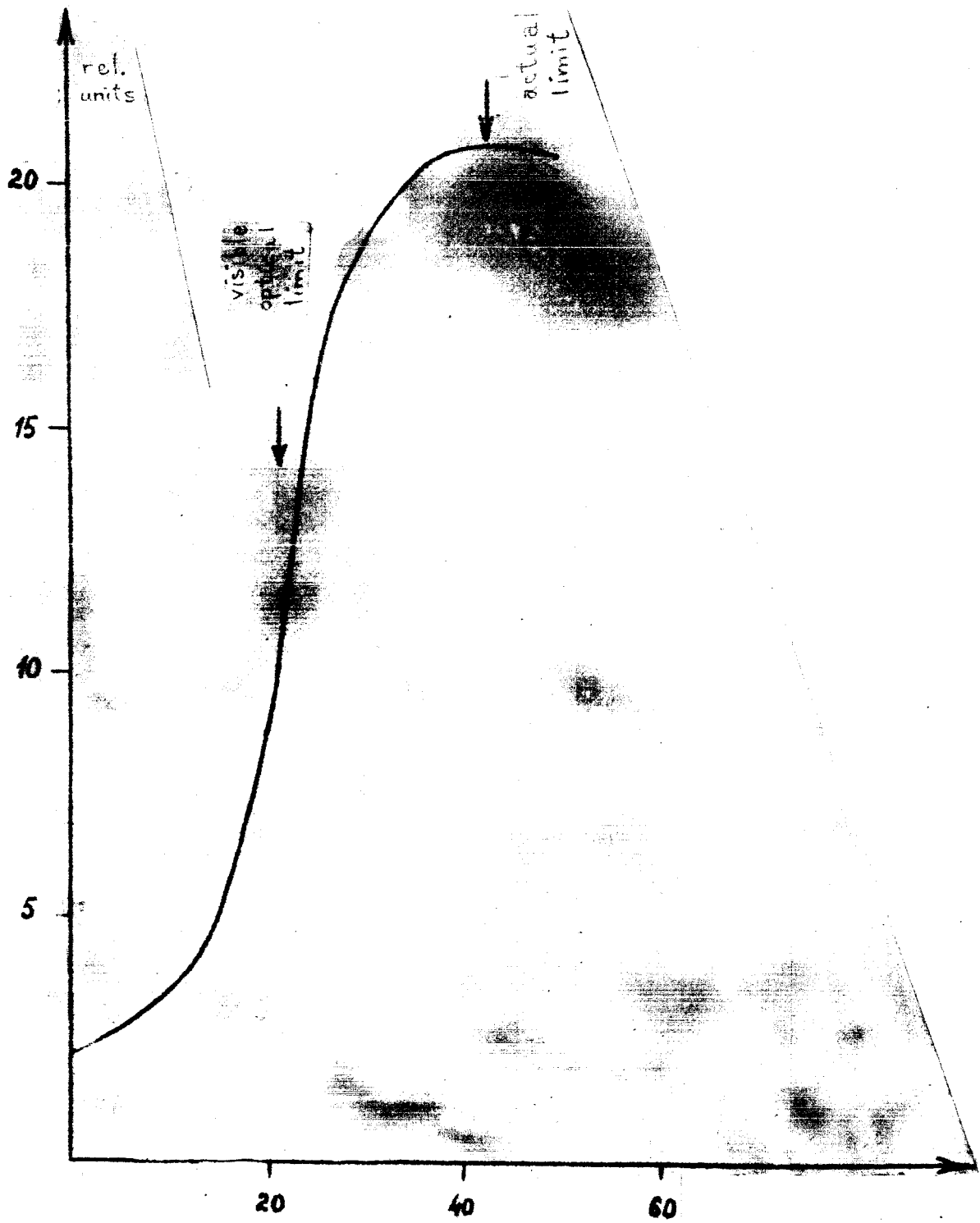
TABLE II

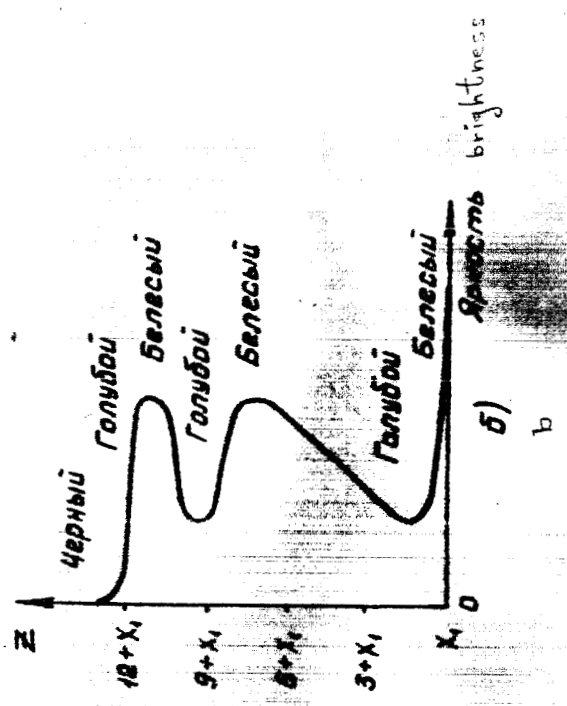
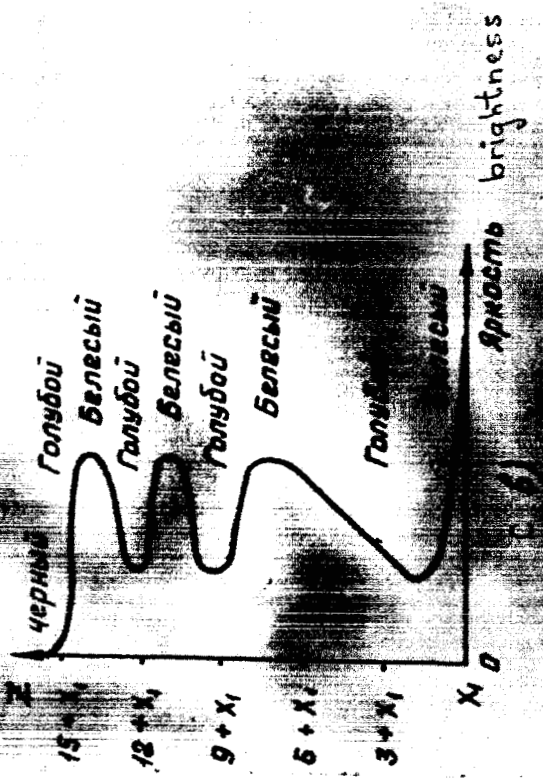
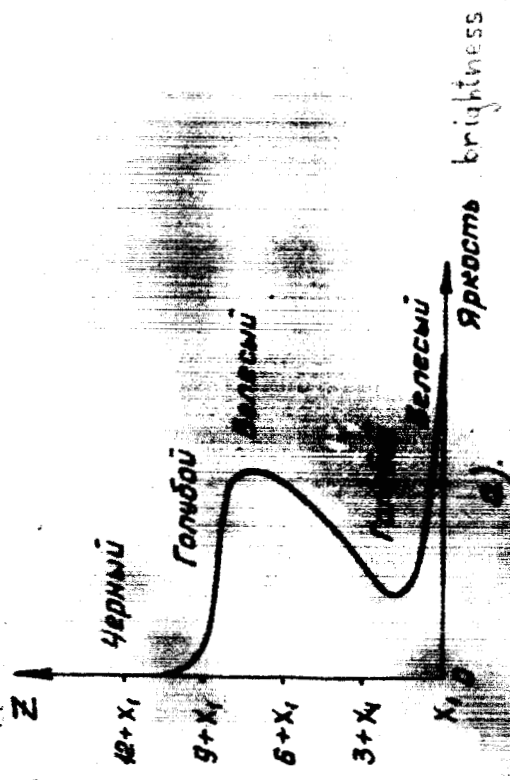
	Relative units					kms.	%%		
	$m(x)$	$D(x)$	$Z(x)$	$Y(x)$	$m(\rho x)$	$m(\tau/30)$ [p(30)]	$m(\tau/4)$ [p(40)]	$m(\tau/50)$ [m(50)]	$1/\alpha$
1)	27,4	6,76	1,49	3,16	0,6	4,0 3,6	-	-	9,0
2)	30,0	10,23	0,80	0,55	1,0	4,7 8,5	-	-	-
3)	41,0	55,86	0,88	1,23	1,2	45,4 0,7	11,4 3,8	6,9 1,7	17,0
4)	42,6	57,26	0,05	0,76	1,2	62,2 0,8	17,9 3,5	7,0 3,7	14,9

For a weak abundance of clouds, the average dimension of heterogeneities of brilliance field is of the order of 8-9 km, for great amounts 12-17.

Figure 14 corresponds to 11a, cloud cover at the periphery of an anti-cyclone.

Figures 10 and 11 show that the separation law in one dimension is never normal. Excess of brilliance is positive for an water surface uncovered and for light nebulosity.





Черный = black
 Голубой = blue
 Белесый = whitish

Figure 1

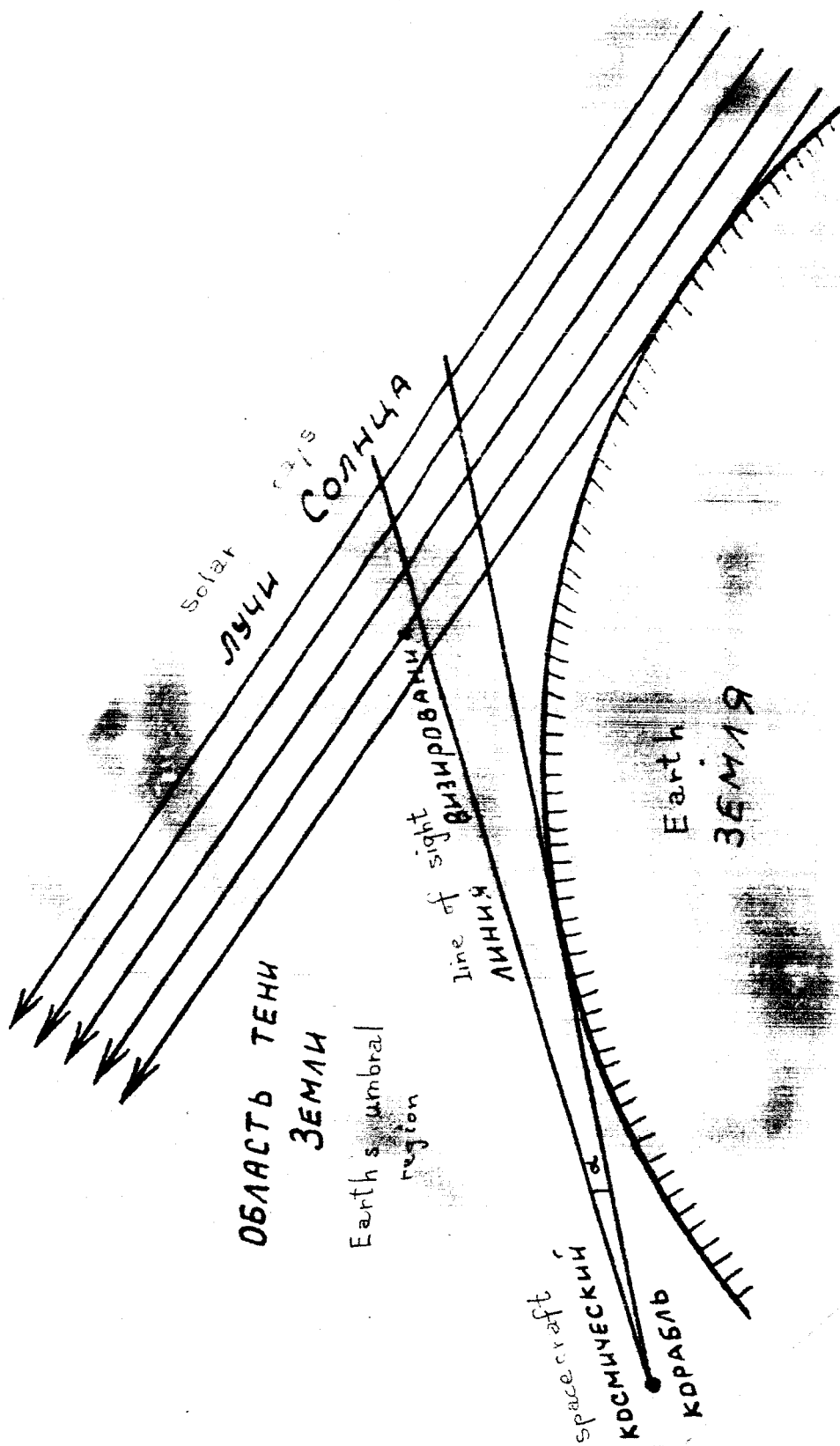
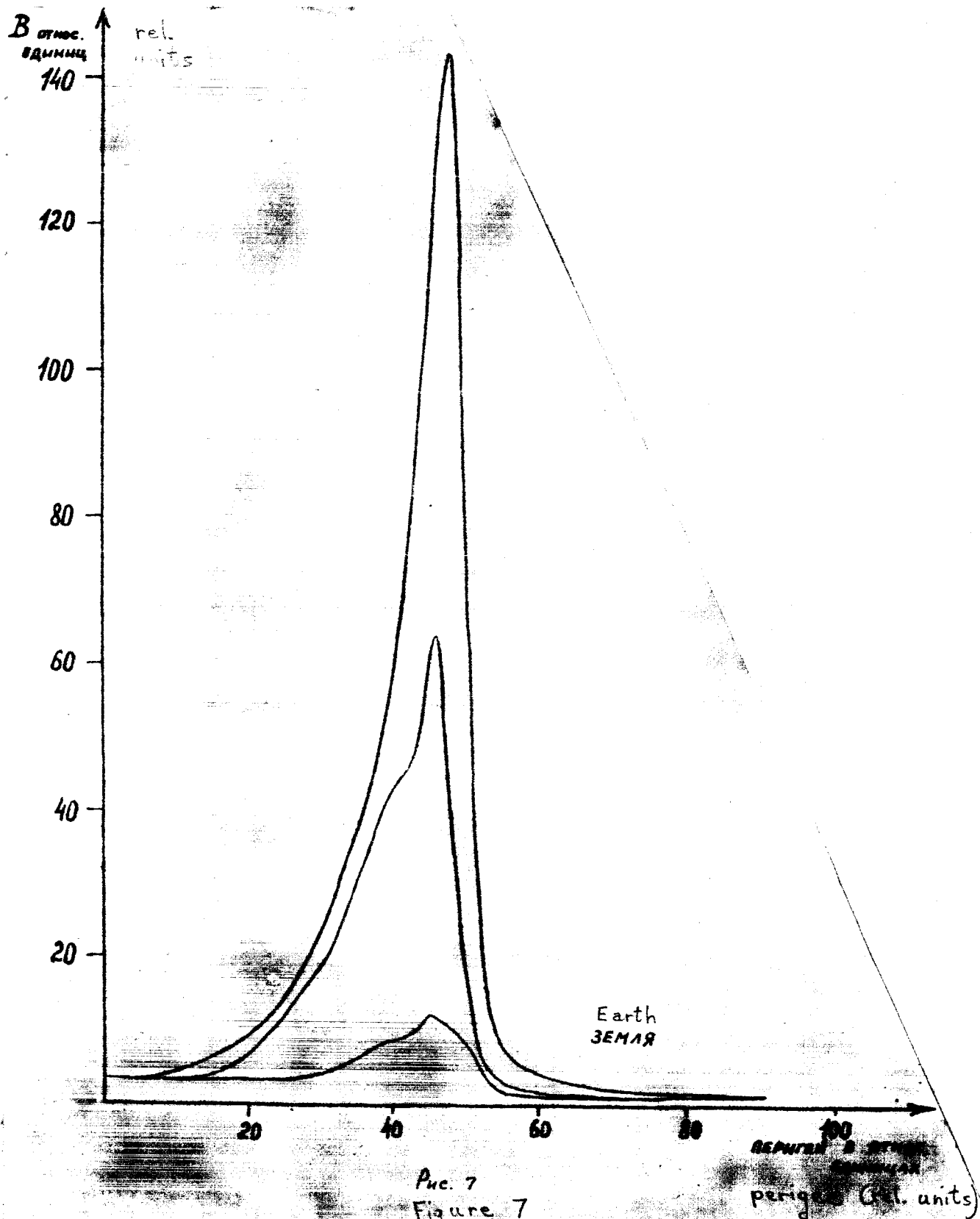


Figure 5

Рис. 5



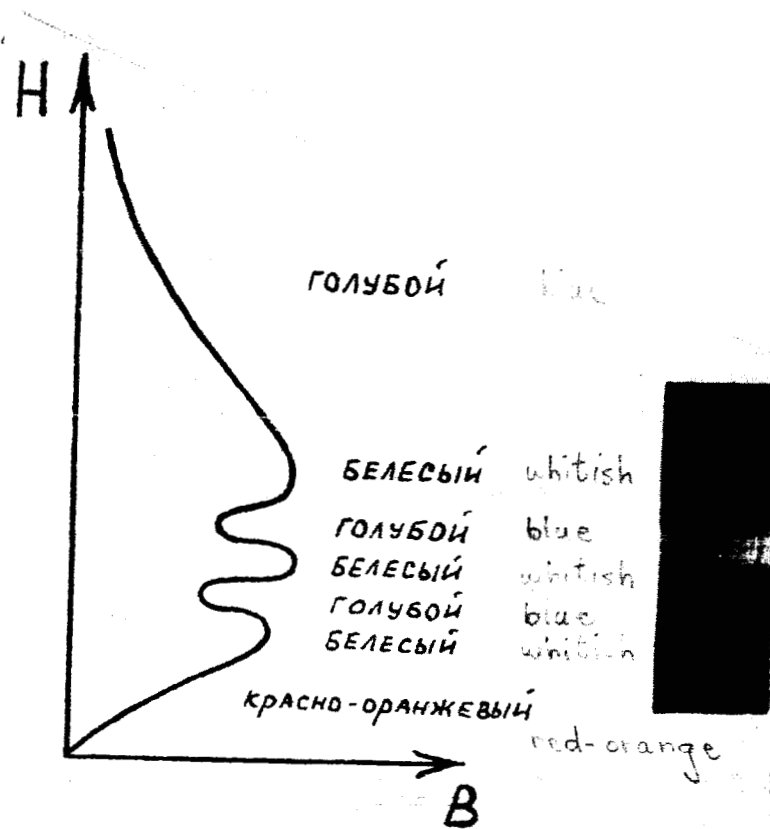


Figure 2
Рис. 8

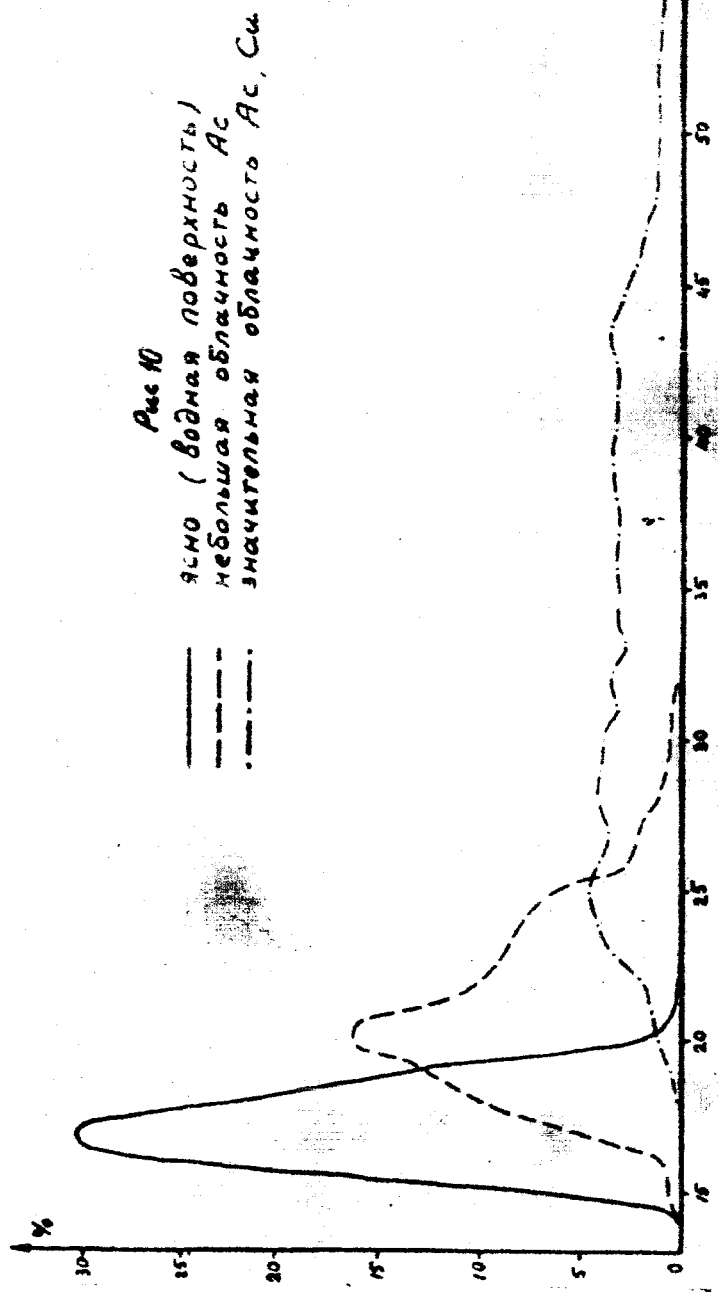


Figure 10
 clear (water surface)
 light cloud cover Ac
 heavy cloud cover As, Cu



Figure 12
 light cloud cover Ac
 heavy cloud cover Ac
 heavy cloud cover Ac, Ci
 heavy cloud cover Ci



%

0.2

0.5

1

2

3

4

5

6

7

8

9

